Pharm Res (2014) 31:861–873
DOI 10.1007/s11095-013-1208-z

RESEARCH PAPER

Effects of Hepatic Ischemia-Reperfusion Injury on the P-Glycoprotein Activity at the Liver Canalicular Membrane and Blood–Brain Barrier Determined by *In Vivo* Administration of Rhodamine 123 in Rats

Mohammad K. Miah • Imam H. Shaik • Ulrich Bickel • Reza Mehvar

Received: 24 April 2013 / Accepted: 12 September 2013 / Published online: 25 September 2013

ABSTRACT

Purpose To investigate the effects of normothermic hepatic ischemia-reperfusion (IR) injury on the activity of P-glycoprotein (P-gp) in the liver and at the blood–brain barrier (BBB) of rats using rhodamine 123 (RH-123) as an *in vivo* marker.

Methods Rats were subjected to 90 min of partial ischemia or sham surgery, followed by 12 or 24 h of reperfusion. Following intravenous injection, the concentrations of RH-123 in blood, bile, brain, and liver were used for pharmacokinetic calculations. The protein levels of P-gp and some other transporters in the liver and brain were also determined by Western blot analysis.

Results P-gp protein levels at the liver canalicular membrane were increased by twofold after 24 h of reperfusion. However, the biliary excretion of RH-123 was reduced in these rats by 26%, presumably due to IR-induced reductions in the liver uptake of the marker and hepatic ATP concentrations. At the BBB, a 24% overexpression of P-gp in the 24-h IR animals was associated with a 30% decrease in the apparent brain uptake clearance of RH-123. The pharmacokinetics or brain distribution of RH-123 was not affected by the 12-h IR injury.

Conclusions Hepatic IR injury may alter the peripheral pharmacokinetics and brain distribution of drugs that are transported by P-gp and possibly other transporters.

KEY WORDS biliary excretion · blood–brain barrier · hepatic ischemia-reperfusion · P-glycoprotein · pharmacokinetics

ABBREVIATIONS

ALT	Alanine aminotransferase
AUC	Area under the plasma concentration-time curve
BBB	Blood–brain barrier
BIBF	Bile salt-independent bile flow
C_{br}^{40}	Concentration in the brain at 40 min
C_{liver}	Concentration in the liver
C_{median}	Concentration in the median lobe of the liver
C_{right}	Concentration in the right lobe of the liver
DTT	DL-dithiothreitol
f_u	Unbound fraction in plasma
IPRL	Isolated perfused rat liver
IR	Ischemia-reperfusion
K_{in}	Apparent brain uptake clearance
LPS	Lipopolysaccharides
Mrp	Multidrug resistance-associated protein
Oatp	Organic anion transporting polypeptide
P-gp	P-glycoprotein
PMSF	Phenylmethanesulfonyl fluoride
RH-110	Rhodamine 110
RH-123	Rhodamine 123
RH-Glu	Rhodamine glucuronide
TNF- α	Tumor necrosis factor-α
UDPGA	Uridine 5′-diphosphoglucuronic acid
$W_{ischemic}$	Weight of ischemic lobes of the liver

M. K. Miah • I. H. Shaik • U. Bickel • R. Mehvar
Department of Pharmaceutical Sciences
Texas Tech University Health Sciences Center
Amarillo, Texas, USA

U. Bickel • R. Mehvar
Center for Blood–Brain Barrier Research
School of Pharmacy, Texas Tech University Health Sciences Center
Amarillo, Texas, USA

R. Mehvar (✉)
School of Pharmacy, Texas Tech University Health Sciences Center
1300 Coulter, Amarillo, Texas 79106, USA
e-mail: reza.mehvar@ttuhsc.edu

Present Address:
I. H. Shaik
School of Pharmacy, University of Pittsburgh
Pittsburgh, Pennsylvania, USA

W_{liver} Total weight of the liver
$W_{non\text{-}ischemic}$ Weight of non-ischemic lobes of the liver

INTRODUCTION

Transient interruption of blood supply to the liver, which occurs in a number of clinical situations such as hypovolemic shock and liver resection surgery or transplantation, causes significant damage to the organ (1–3). Ironically, reperfusion of the liver, following re-establishment of blood supply to the ischemic liver, enhances this injury via different mechanisms. For instance, gut-derived lipopolysaccharides (LPS) are translocated directly into the liver circulation during the reperfusion period (4), activating the liver Kupffer cells. Activation of Kupffer cells results in the production and release of proinflammatory mediators, such as reactive oxygen species, high mobility group protein B1, and cytokines, including tumor necrosis factor (TNF)-α, interleukin-1β, and interleukin-6 (3,5–8). Among these proinflammatory mediators, cytokines are known to alter hepatic transporters, such as sodium taurocholate cotransporting polypeptides, P-glycoprotein (P-gp), organic anion transporting polypeptides (Oatp), and multidrug resistance-associated proteins (Mrp) at the mRNA and/or protein levels (9–11). Additionally, previous studies (8,12–14) have shown that hepatic ischemia-reperfusion (IR) injury alters the mRNA and/or protein levels of sinusoidal and canalicular liver transporters. However, very little is known about the effects of hepatic IR-induced changes in the mRNA and/or protein levels of transporters on the hepatobiliary disposition (15) or *in vivo* pharmacokinetics (12) of drugs.

In addition to the transporters in the liver, hepatic IR may potentially alter the expression of transporters in remote organs via the release of proinflammatory mediators into the circulation. Indeed, Tanaka *et al.* (13) recently reported that whereas hepatic IR injury in rats decreased the mRNA and protein levels of Mrp2 in the liver, it upregulated the transporter's expression in the kidneys. The authors suggested that the increased Mrp2 expression in the kidney might be a protective mechanism in response to the downregulation of the transporter in the liver. Further, a recent study (12) showed that hepatic IR injury in rats resulted in upregulation of P-gp in the upper intestine, partially responsible for a lower oral bioavailability of cyclosporine A observed in the rats subjected to the hepatic IR injury. Therefore, hepatic IR injury may affect the pharmacokinetics of drugs by affecting transporters in both the liver and remote organs.

Among ATP-binding cassette transporters, P-gp plays a major role in the biliary excretion of many drugs. Additionally, P-gp is an important gatekeeper at the blood–brain barrier (BBB) of many species (16). At the BBB, P-gp is located at the luminal (blood) side of the brain capillary endothelium, pumping a variety of substrates back into the blood, thus limiting their access to brain tissue (17–20). Therefore, situations that change the function of P-gp at the BBB are of significant clinical importance in terms of both drug delivery to the brain and neurotoxicity.

The goal of the current study was to study the effects of hepatic IR injury on the P-gp expression and function in the liver itself and at the BBB as a remote structure. To study the function of P-gp *in vivo*, we selected rhodamine-123 (RH-123), which is a well-established P-gp substrate. Indeed, *in vivo* administration of RH-123 has been used before as a marker for detection of P-gp function both at the liver canalicular interface (21) and BBB (22,23). Additionally, the glucuronidated metabolite of the marker (RH-Glu) is a selective substrate for Mrp2 (24,25), which allows determination of the function of Mrp2 in addition to that of P-gp after the administration of RH-123.

MATERIALS AND METHODS

Chemicals and Reagents

RH-123, 7-hydroxycoumarin, d-saccharolactone, β-glucuronidase (Type-LII), and uridine 5′-diphosphoglucuronic acid (UDPGA) were obtained from Sigma–Aldrich (St. Louis, MO, USA). Ketamine and xylazine solutions for anesthesia were purchased from Lloyd Laboratories (Shenandoah, IA, USA), and heparin solution was obtained from APP Pharmaceuticals (Schaumburg, IL, USA). NADPH was obtained from Calzyme Lab Inc. (San Luis Obispo, CA, USA). Mouse monoclonal anti-P-gp antibody was from Calbiochem (Gibbstown, USA), anti-Mrp2 antibody was from Enzo life Sciences (Plymouth meeting, PA, USA), anti-β-actin antibody was from Sigma-Aldrich, and Rabbit polyclonal anti-Oatp1a4 antibody was from LSBio (Seattle, WA, USA). Alanine aminotransferase (ALT) kits were from Teco Diagnostics (Anaheim, CA, USA). BCA kit for the measurement of protein was purchased from Pierce Biotechnology (Rockford, IL, USA). All other chemicals were analytical grade and obtained from commercial sources.

Animals

The Institutional Animal Care and Use Committee approved the use of animals in this study, and the procedures involving animals were consistent with the guidelines set by National Institute of Health (NIH publication #85-23, revised in 1985). Adult, male Sprague–Dawley rats (225–300 g) were purchased from Charles River Laboratories, Inc. (Wilmington, MA, USA). All the animals were acclimatized in animal care facility for at least 2–4 days before surgery, with free access to regular food and water.

Hepatic Ischemia-Reperfusion Model

We used a well-established partial (70%) ischemia-reperfusion model, which has been described in detail before (26–28). Both ischemia and the following reperfusion contribute to the IR injury in this model. Briefly, after an overnight fast, animals were anesthetized by an intramuscular injection of a mixture of ketamine: xylazine (80:8 mg/kg body weight), and the abdomen was opened. To induce ischemia, the blood supplies to the median and left lobes were completely interrupted for 90 min. Because of the significant effect of temperature on the outcome of IR injury, the body temperature of rats was strictly maintained at 37°C by using a combination of a heat lamp and a heating plate controlled by a rectal temperature probe during the surgery. At the end of the ischemic period, the blood flow to the ischemic lobes was reinstated. To compensate for any water loss during the ischemic period, 5 ml of warm (37°C) sterile saline was added into the abdomen before closure of the incision. Sham-operated animals underwent laparatomy without ischemia under the same surgical condition as in the IR group. Different groups of animals ($n = 5–9$/group) were used 12 or 24 h after the reinstatement of the blood flow or sham surgery. Therefore, the IR injury in this study refers to a combination of 90 min of ischemia and 12 or 24 h of reperfusion. The sample size for the 24-h groups ($n = 9$) was estimated based on the magnitude of difference between the 24-h sham and IR groups and variability in the biliary excretion of RH-123 observed in isolated perfused rat livers (15). In the absence of previous data on the expected magnitude of difference between the sham and IR in the 12-h groups, 5 animals were used for these groups.

Dosing and Sample Collection

After 12 or 24 h of reperfusion or sham surgery, rats were anesthetized, and catheters were inserted into the bile duct and jugular vein to collect bile and blood, respectively. After intravenous bolus administration to rats, RH-123 follows a three-exponential kinetic model (29), resulting in a rapid decline in its early plasma concentrations. To avoid substantial fluctuations in the plasma concentrations of RH-123, which may potentially result in nonlinearity in the transport of the drug, RH-123 was infused into the penile vein at a constant rate of 12.5 μg/kg/min over 40 min (total dose of 500 μg/kg). Serial (0, 5, 10, 20, 30, and 40 min) blood samples (~250 μl each) were then collected in heparinized microcentrifuge tubes from the jugular vein catheter. To prevent clotting, the catheter was filled with a heparin (10 U/ml) solution in saline. Blood samples were centrifuged immediately, and plasma was separated. Cumulative bile (0–40 min) was also collected. At the end of the experiment, a small piece of liver from the left lobe was cut and immediately (≤3 s) frozen in liquid nitrogen for measurement of ATP levels. Subsequently, the vasculature blood was flushed out with 50 ml of ice-cold saline delivered at a flow rate of 25 ml/min through a catheter inserted into the left ventricle of the heart, and brain and liver tissue were collected. After snap-freezing the brain and liver in dry ice/isopentane and liquid nitrogen, respectively, the samples were stored at −80°C for subsequent analysis.

Analysis of RH-123 and its Metabolites

Liver samples were homogenized in deionized water (1:9) and after an additional five-fold dilution with 2% (w/v) albumin were used in the assay. The concentrations of RH-123 and its metabolites were measured in both ischemic (median) and non-ischemic (right) lobes separately. Brain samples were homogenized in deionized water (1:4) before analysis. Finally, bile samples were diluted 50 times with the 2% albumin solution before analysis. The plasma samples were measured without dilution. The concentrations of RH-123 and its metabolite RH-110 in the samples were quantitated by modifications of an HPLC method described before (30). Briefly, 50 μl of each sample was thoroughly mixed with 50 μl of deionized water before the addition of 100 μl of ice-cold acetonitrile for protein precipitation. Following vortex-mixing and centrifugation, 50 μl of clear supernatant was injected onto HPLC for analysis at excitation and emission wavelengths of 505 and 525 nm, respectively. The calibration standards were constructed in the range of 6.25–500 (RH-123) and 1.25–100 (RH-110) ng/ml for plasma, 5–250 (RH-123) and 1–50 (RH-110) ng/ml for liver homogenates, 5–200 (RH-123) and 1–40 (RH-110) ng/ml for bile, and 0.25–10 (RH-123) and 0.05–2 (RH-110) ng/ml for brain homogenates. The inter-day CV values (%) of the slopes ($n = 4$) were 10.1 (RH-123) and 4.17 (RH-110) for plasma, 10.1 (RH-123) and 4.26 (RH-110) for liver, 2.23 (RH-123) and 0.84 (RH-110) for bile, and 7.50 (RH-123) and 8.56 (RH-110) for brain samples.

For the bile samples, the concentrations of RH-123 were analyzed both before and after treatment with β-glucuronidase to estimate the RH-Glu concentrations (30). Preliminary studies showed that the concentrations of RH-Glu in the plasma, liver, and brain samples were negligible, if any. Therefore, for these samples, only the unhydrolyzed samples were analyzed.

Analysis of ALT

Plasma ALT levels were measured spectrophotometrically using a commercially available kit.

Analysis of Unbound Fraction of RH-123 and RH-110 in Plasma

The degree of binding of RH-123 or RH-110 to plasma proteins was determined by ultrafiltration method using Microcon Ultracel YM-30 centrifugal devices, with a MWCO of 30 K, from Millipore (Billerica, MA, USA). To prevent adsorption of analytes to the membrane and/or device, the device was pretreated with 5% benzalkonium chloride as described before (31). Approximately, 100 µl of the terminal (40 min) plasma sample was added to the device, which was then incubated at 37°C for 30 min before centrifugation at 2000 g for 15 min (37°C). Aliquots (10 µl) of the original plasma samples and the filtrate were then subjected to the HPLC assay described above. The free fraction (f_u) of RH-123 or RH-110 was estimated by dividing the analyte concentration in the filtrate by that in the original plasma sample.

Measurement of Hepatic ATP Levels

The concentrations of ATP in the samples from the left lobes of the livers were analyzed by a reversed-phase, gradient HPLC method as described before (32).

7-Hydroxycoumarin (Umbelliferone) Glucuronidation Assay

To determine the glucuronidation capacity of the liver, umbelliferone (7-hydroxycoumarin) was used as a substrate marker for uridine diphosphate glucuronosyltransferase using a method described before (33). Briefly, liver samples from the median lobes were homogenized in cold, pH 7.4 PBS (1:80), and protein concentrations were measured by the BCA kit. The reaction mixture (500 µl) contained liver homogenate (1 mg protein/ml), 100 µM 7-hydroxycoumarin, 6.25 mM magnesium chloride, 6.25 mM D-saccharolactone, and 1.25 mM UDPGA in PBS (pH 7.4). The reaction mixture without UDPGA was preincubated at 37°C for 10 min before starting the reaction by the addition of UDPGA. After incubation at 37°C for 20 min, the reaction was terminated by the addition of 500 µl of 0.4 M perchloric acid. After mixing and centrifugation, the supernatant was subjected to an HPLC analysis for the measurement of umbelliferone and its glucuronide (34). The glucuronidation capacity was expressed as percentage of the initial umbelliferone converted to umbelliferone glucuronide.

Western Blot Analysis

Analysis was conducted on crude membrane fractions, which were prepared based on standard methods. Briefly, liver (left lobe) and brain samples were homogenized in a homogenization buffer (1:4), which contained 10 mM Tris–HCl pH 7.4, 1 mM EGTA, 1 mM $MgCl_2$, 1 mM mercaptoethanol, 1 mM DTT, 2 mM PMSF, and 1% glycerol. To 1 ml of homogenate were added 40 µl of 0.5 M Tris–HCl and 1 µl of protease inhibitor cocktail for mammalian cells and tissue extracts (Sigma), and the samples were centrifuged (4°C) at 2000 g for 15 min. The supernatant was separated and centrifuged (4°C) at 100,000 g for 30 min to obtain the membrane fraction. The pellets were re-suspended in 250 µl of homogenization buffer containing 2.5 µl of the protease inhibitor PMSF (100 mM), and the protein concentrations were measured by the BCA kit. Membrane fractions from the brain (40 µg) and liver (30 µg) samples were then resolved by 4–20% gradient SDS-polyacrylamide gel electrophoresis (Thermo Scientific, Rockford, IL, USA) for the analysis of the brain P-gp and Oatp1a4 and liver P-gp and Mrp2. Additionally, an 8% SDS gel was used for the analysis of liver Oatp1a4. The proteins were then transferred to a PVDF membrane (Bio-Rad, Hercules, CA, USA), and the membrane was stained with Ponceau S. After blocking the membranes with 5% albumin, they were incubated overnight (4°C) with primary antibodies against P-gp, Mrp2, or Oatp1a4. Additionally, incubation with β-actin antibody was used for loading control. Finally, the membranes were treated with anti-mouse or anti-rabbit horseradish peroxidase-conjugated secondary antibodies, and band intensities were quantified using VersaDoc Image system and Quantity One software (Bio-Rad).

Pharmacokinetic Analysis

The area under the plasma concentration-time curve from 0 to 40 min ($AUC_{0\text{-}40}$) for RH-123 was calculated using the linear trapezoidal method. The total liver concentrations (C_{liver}) of RH-123 and its metabolites were estimated using the following equation:

$$C_{liver} = \frac{(C_{median} \times W_{ischemic}) + (C_{right} \times W_{non-ischemic})}{W_{liver}}$$

where C_{median} and C_{right} are the concentrations in the median and right lobes, and $W_{ischemic}$, $W_{non\text{-}ischemic}$, and W_{liver} are the weight of ischemic lobes (median and left), non-ischemic lobes (right and caudate), and whole liver, respectively. This calculation assumes that C_{median} and C_{right} are representative of the concentrations in the ischemic (median and left) and non-ischemic (right and caudate) lobes. Apparent biliary clearance of RH-123 was estimated by dividing the amount of RH-123 excreted into bile over 40 min by the $AUC_{0\text{-}40}$. The apparent brain uptake clearance (K_{in}) of RH-123 was calculated from the plasma $AUC_{0\text{-}40}$ and the terminal brain concentration of RH-123 at 40 min (C_{br}^{40}) according to the following equation (35):

$$K_{in} = \frac{C_{br}^{40}}{AUC_{0-40}}$$

Statistical Analysis

The results are expressed as mean ± SD. All statistical analyses were performed using GraphPad Prism version 6.00 (GraphPad Software, San Diego, CA). Differences between the Sham and IR groups in terms of plasma concentrations of RH-123 and RH-110 at different time points were analyzed by a repeated-measure, two-way ANOVA, followed by Bonferroni's multiple comparison of the means. The differences between the Sham and IR groups in terms of other parameters were assessed by an unpaired student *t*-test when the variances of the two samples were the same. In the presence of significant differences between the variances of the IR and Sham groups, Welch's correction was applied. The threshold of the significance was $p < 0.05$.

RESULTS

Plasma Concentrations of ALT

The plasma concentrations of ALT in both 12 and 24 h IR groups were significantly higher than those in their corresponding Sham groups (12-h groups: 667 ± 292 IU/l *versus* 137 ± 41 IU/l, $p < 0.01$; 24-h groups: 867 ± 467 IU/l *versus* 66.5 ± 31.8 IU/l, $p < 0.001$), which confirms substantial damage to the liver due to the IR injury.

Plasma Pharmacokinetics

Although the concentrations of RH-123 and its deacylated metabolite, RH-110, were measurable in all the plasma samples, the concentrations of RH-Glu were negligible in most of the plasma samples during the 40-min infusion of the drug. The plasma concentration-time courses of RH-123 and RH-110 after 12 or 24 h of IR surgery or sham operation are presented in Fig. 1. Despite the constant intravenous infusion of the drug, the plasma concentrations of RH-123 and its metabolite RH-110 did not reach plateau in most groups during the 40 min of the infusion, an observation that was more evident for the metabolite (Fig. 1). The plasma concentrations of RH-123 after 12 h of IR injury were not significantly different from those in the Sham group (Fig. 1a). However, 24 h of IR caused a significant increase in the plasma concentrations of RH-123 at all the time points except for the 5 min sample (Fig. 1b). As for RH-110, neither 12 nor 24 h of IR had any significant impact on its plasma concentration-time course (Fig. 1c and d).

The plasma AUC and f_u values of RH-123 and RH-110 are listed in Table I. In agreement with the plasma concentration-time data (Fig. 1), there was no significant difference between the AUC of RH-123 in the IR and Sham groups after 12 h of reperfusion. However, the RH-123 AUC in the IR group after 24 h of reperfusion was 56% higher ($p < 0.01$) than that in its corresponding Sham group (Table I). The AUC values for RH-110 were similar in the Sham and IR groups after either 12 or 24 h of reperfusion (Table I). Additionally, the RH-110:RH-123 AUC ratio in the 24 h IR rats (0.122 ± 0.024) was significantly ($p < 0.01$) lower than that in the Sham group (0.157 ± 0.020), suggesting an IR-induced reduction in the formation of RH-110 from RH-123 after 24 h of reperfusion. IR did not affect the plasma free fractions of either RH-123 or its metabolite RH-110. However, the free fraction of RH-110 was significantly higher than that of RH-123 within each group (Table I).

Biliary Excretion

The biliary recoveries of RH-123 and RH-Glu along with the apparent biliary clearance of RH-123 and bile flow rates are presented in Fig. 2 for both the 12- (Fig. 2a-d) and 24- (Fig. 2e-h) h reperfusion groups. After 12 h of reperfusion, there were no significant differences between the Sham and IR groups in any of the biliary parameters (Fig. 2a-d). However, 24 h of IR resulted in significant differences in all the measured parameters (Fig. 2e-h), which are explained here in more detail. The biliary recovery (Fig. 2e) and apparent clearance (Fig. 2f) values of RH-123 in the IR group were 26% ($p < 0.05$) and 45% ($p < 0.01$) lower, respectively, as compared with the corresponding values in the Sham group. Additionally, 24-h IR caused a 53% decrease ($p < 0.01$) in the biliary recovery of RH-Glu (Fig. 2g). Lastly, bile flow rates in the 24-h IR group were 30% lower ($p < 0.001$) than those in the Sham group (Fig. 2h). In contrast to RH-123 and RH-Glu, the biliary recovery of RH-110 (~0.02% of the dose) was negligible (data not shown).

Brain Uptake

The brain concentrations and apparent uptake clearance (K_{in}) values of RH-123 and RH-110 are presented in Fig. 3 for both the 12- (Fig. 3a-d) and 24- (Fig. 3e-h) h reperfusion groups. After 12 h of reperfusion, there were no significant differences between the Sham and IR groups in their brain concentrations or K_{in} values of RH-123 or RH-110 (Fig. 3a-d). As for the 24-h reperfusion groups, despite substantially higher plasma concentrations in the IR group (Fig. 1b), the brain concentrations of RH-123 in the IR and Sham groups were not significantly different (Fig. 3e). This was due to ~30% lower ($p < 0.05$) K_{in} for RH-123 in the IR animals (Fig. 3f). In contrast to RH-123, although 24-h IR did not significantly affect the brain K_{in} of RH-110 (Fig. 3h), the brain concentrations of the metabolite in the IR rats were significantly ($p < 0.05$) higher than those in the Sham animals (Fig. 3g).

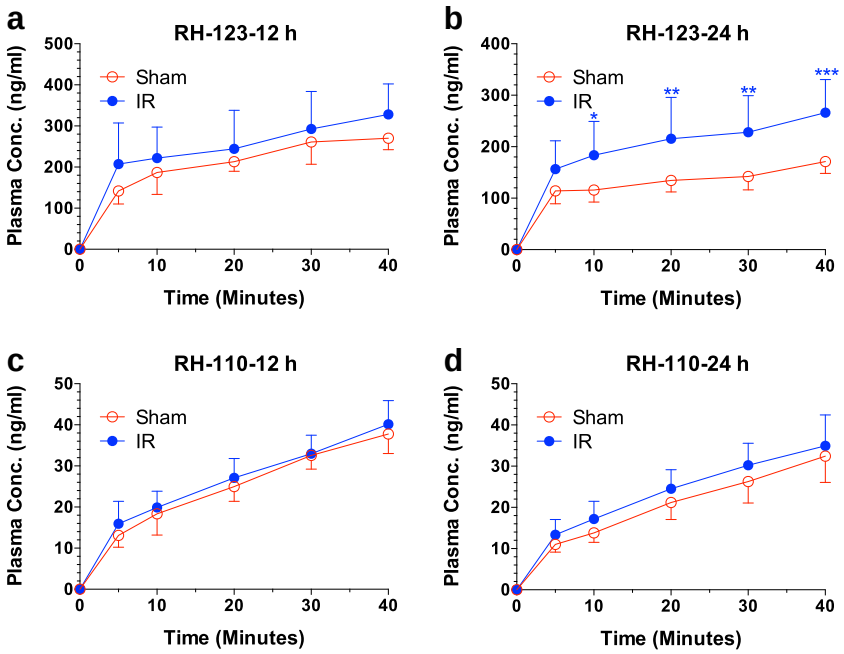

Fig. 1 Plasma concentration-time courses of RH-123 (**a** and **b**) and RH-110 (**c** and **d**) in rats subjected to partial hepatic ischemia (IR) or sham operation (Sham) and 12 (**a** and **c**) or 24 (**b** and **d**) h of reperfusion. RH-123 was infused intravenously at a constant rate of 12.5 μg/kg/min over 40 min. *Symbols* and *bars* represent mean and SD values, respectively. Animal numbers were 5 and 6 for the Sham and IR animals, respectively, in the 12 h group and 9 for either Sham or IR animals in the 24 h group. * $p < 0.05$, ** $p < 0.01$, *** $p < 0.001$: Significant difference between the Sham and IR at each time point based on repeated-measure, two-way ANOVA, followed by Bonferroni's post-hoc analysis.

Mechanistic Studies

To gain insight into the reasons behind changes in the biliary excretion of RH-123 and RH-Glu and brain K_{in} of RH-123 after 24 h of reperfusion, additional studies were conducted using the liver and brain samples from these groups. Figure 4 demonstrates the amount of RH-123 recovered in the liver (Fig. 4a), RH-123 liver: plasma concentration ratio (Fig. 4b), the liver concentrations of ATP (Fig. 4c), and the extent of umbelliferone glucuronidation by the liver homogenates (Fig. 4d). Substantial amounts of RH-123 (~25% of the dose) were found in the liver of Sham rats after 40 min of drug infusion (Fig. 4a). However, despite the higher plasma concentrations (Fig. 1b) and AUC values (Table I) in the IR group, the liver concentrations and amounts of RH-123 in the Sham and IR rats were not significantly different (Fig. 4a). Consequently, the terminal liver: plasma concentration ratios of RH-123 in the IR group were 29% lower ($p < 0.01$) than those in the Sham group (Fig. 4b). No RH-Glu was measurable in the liver samples, and the concentrations of RH-110 in the liver were ≤10% of those of RH-123 (data not shown). Additionally, the liver concentration of ATP in the IR group

Table I Plasma Pharmacokinetic Parameters (Mean ± SD) of RH-123 and its Metabolites RH-110 After Constant Intravenous Infusion of RH-123 (12.5 μg/kg/min) for 40 min in Rats Subjected to Partial Hepatic Ischemia (IR) or Sham Surgery (Sham) and 12 or 24 h of Reperfusion

Treatment	AUC, ng.min/ml			f_u	
	RH-123	RH-110	RH-110:RH-123 Ratio	RH-123	RH-110
12-h groups					
Sham ($n = 5$)	8210 ± 1160	968 ± 138	0.119 ± 0.016	0.302 ± 0.020	0.379 ± 0.058¶
IR ($n = 6$)	9710 ± 3060	1030 ± 166	0.111 ± 0.020	0.300 ± 0.019	0.389 ± 0.037¶¶¶
24-h groups					
Sham ($n = 9$)	5070 ± 785	795 ± 142	0.157 ± 0.020	0.270 ± 0.029	0.340 ± 0.044¶¶
IR ($n = 9$)	7930 ± 2500**	918 ± 174	0.122 ± 0.024**	0.264 ± 0.032	0.346 ± 0.0700¶¶

** $p < 0.01$: Significantly different from the corresponding Sham group (unpaired t test)

¶ $p < 0.05$, ¶¶ $p < 0.01$, ¶¶¶ $p < 0.001$: Significantly different from RH-123 (unpaired t test)

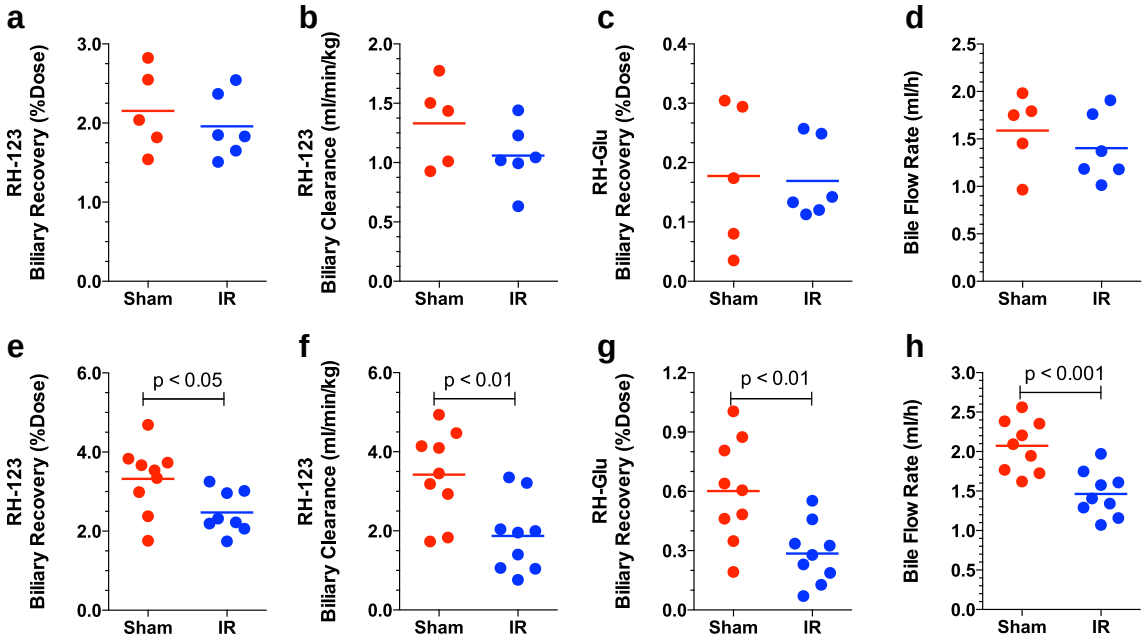

Fig. 2 Biliary recovery of RH-123 (**a** and **e**), apparent biliary clearance of RH-123 (**b** and **f**), biliary recovery of RH-Glu (**c** and **g**), and bile flow rates (**d** and **h**) in rats subjected to partial hepatic ischemia (IR) or sham operation (Sham) and 12 (**a**-**d**) or 24 (**e**-**h**) h of reperfusion. RH-123 was infused intravenously at a constant rate of 12.5 μg/kg/min over 40 min. *Symbols* represent individual animals.

was 23% lower ($p < 0.05$) than that in the Sham group (Fig. 4c). However, the extents of umbelliferone glucuronidation, a marker for the glucuronidation capacity of the liver, in the Sham and IR livers were not different from each other (Fig. 4d).

We also measured the protein levels of P-gp, Mrp2, and Oatp1a4 in the liver membrane fractions. The representative Western blots and individual densitometric data for the three studied hepatic transporters are presented in Fig. 5. Whereas IR caused an almost twofold increase ($p < 0.05$) in the protein

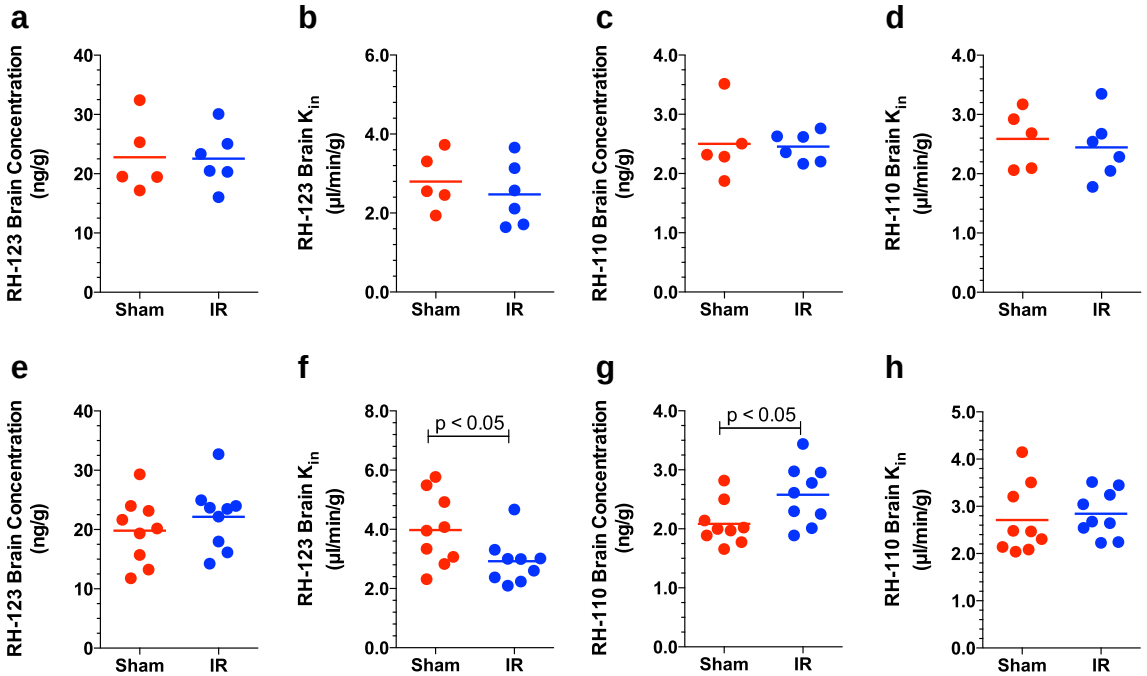

Fig. 3 Brain concentrations of RH-123 (**a** and **e**), apparent brain uptake clearance (K_{in}) of RH-123 (**b** and **f**), brain concentrations of RH-110 (**c** and **g**), and apparent brain uptake clearance (K_{in}) of RH-110 (**d** and **h**) in rats subjected to partial hepatic ischemia (IR) or sham operation (Sham) and 12 (**a**-**d**) or 24 (**e**-**h**) h of reperfusion. RH-123 was infused intravenously at a constant rate of 12.5 μg/kg/min over 40 min. *Symbols* represent individual animals.

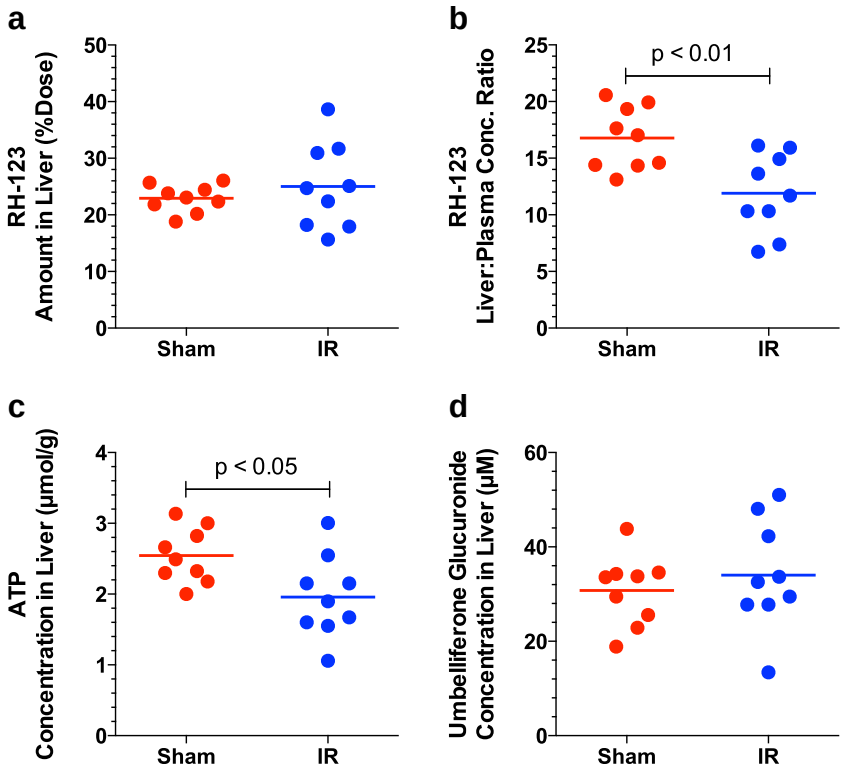

Fig. 4 Amount of RH-123 recovered in the terminal liver sample (**a**), terminal liver: plasma concentration ratio of RH-123 (**b**), hepatic concentration of ATP (**c**), and extent of formation of umbelliferone glucuronide in the liver homogenate (**d**) in rats subjected to partial hepatic ischemia (IR) or sham operation (Sham), followed by 24 h of reperfusion. RH-123 was infused intravenously at a constant rate of 12.5 $\mu g/kg/min$ over 40 min. *Symbols* represent individual animals.

expression of P-gp in the liver membrane fractions (Fig. 5a), the protein contents of Mrp2 and Oatp1a4 were down-regulated by 46% ($p < 0.01$) (Fig. 5b) and 28% ($p < 0.05$) (Fig. 5c), respectively, as a result of the IR injury.

Finally, we determined the protein levels of P-gp and Oatp1a4 in the brain membrane fractions. The representative Western blots and individual densitometric data for these brain transporters are presented in Fig. 6. The brain P-gp protein levels in the IR group were 24% higher ($p < 0.05$) than those in the Sham group (Fig. 6a). However, the Oatap1a4 protein levels in the IR and sham groups (Fig. 6b) were not significantly different ($p = 0.066$).

DISCUSSION

In one of the original reports on the effects of hepatic IR injury on the liver transporters, Tanaka *et al.* (8) showed that whereas the injury decreased the mRNA of a number of sinusoidal transporters and Mrp2, the mRNA of Mdr1b was significantly

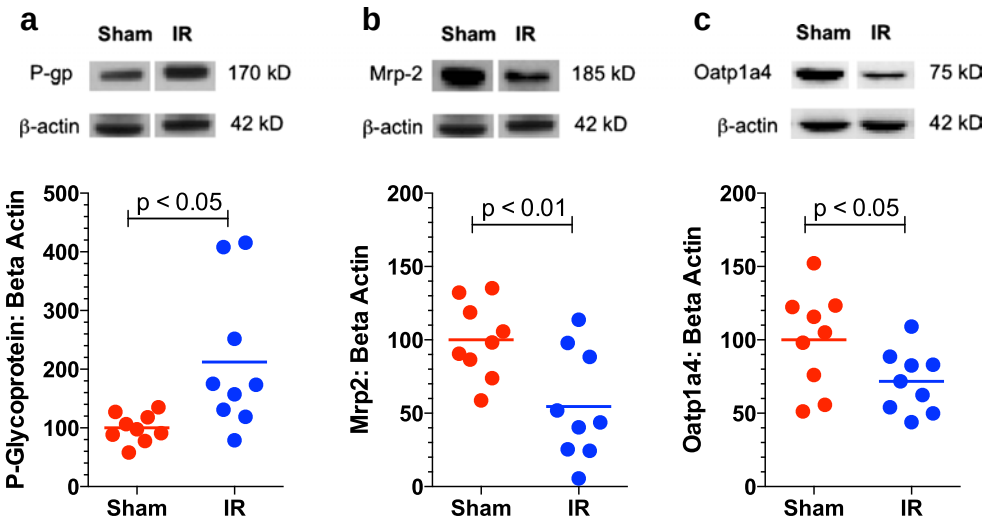

Fig. 5 Representative Western blots (*top* panels) and individual densitometric data (*bottom* panels) for P-gp (**a**), Mrp2 (**b**), and Oatp1a4 (**c**) in the liver membrane fractions from rats subjected to partial hepatic ischemia (IR) or sham operation (Sham), followed by 24 h of reperfusion. RH-123 was infused intravenously at a constant rate of 12.5 $\mu g/kg/min$ over 40 min. *Symbols* represent individual animal data, which are normalized based on the Sham values (100%).

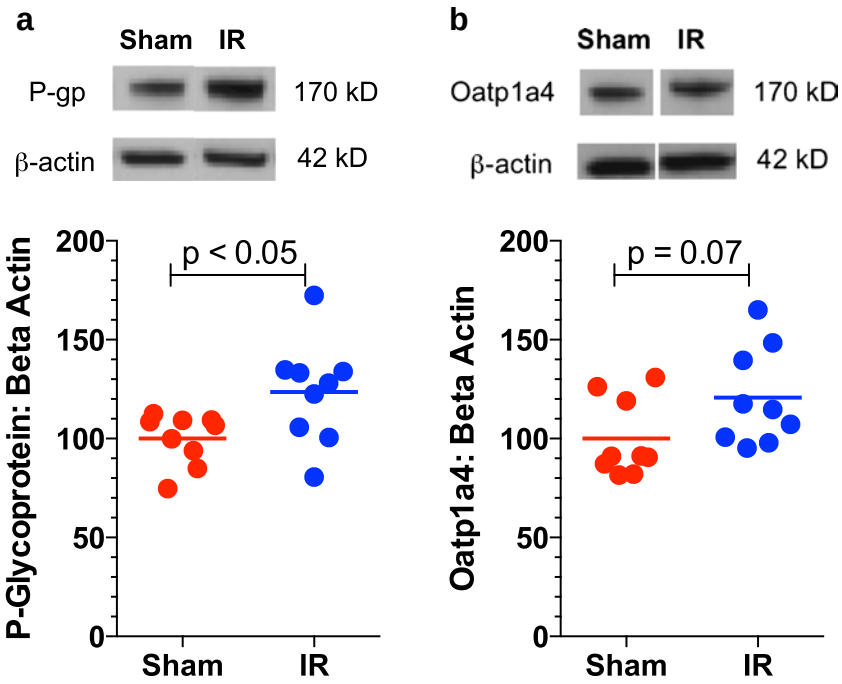

Fig. 6 Representative Western blots (*top* panels) and individual densitometric data (*bottom* panels) for P-gp (**a**) and Oatp1a4 (**b**) in the brain membrane fractions from rats subjected to partial hepatic ischemia (IR) or sham operation (Sham), followed by 24 h of reperfusion. RH-123 was infused intravenously at a constant rate of 12.5 μg/kg/min over 40 min. *Symbols* represent individual animal data, which are normalized based on the Sham values (100%).

upregulated 24 h after the injury in rats. In a agreement with that report, a subsequent study (12) revealed that the protein levels of P-gp were modestly (~20%) increased after the hepatic IR injury in rats. Very recently (15), we investigated the potential effects of hepatic IR-induced increase in P-gp mRNA and protein levels on the biliary excretion of RH-123, a well-established marker of P-gp, in an isolated perfused rat liver (IPRL) model. However, in contrast to the reported increases in the mRNA (8) and protein (12) levels of P-gp, the biliary excretion of RH-123 significantly decreased 24 h after the IR injury (15). Although several possible explanations were provided, the reason(s) for this apparent discrepancy remained unclear. Therefore, one of the goals of the present *in vivo* study was to clarify this apparent discrepancy.

Similar to the previous IPRL study (15), 24-h IR caused significant reductions in the biliary excretion (Fig. 2e) and apparent clearance (Fig. 2f) of RH-123 in the present *in vivo* study. However, additional mechanistic studies presented here (Figs. 4b, c and 5a, c) provide some insights into the apparent discrepancy between the expression and function of the canalicular P-gp as a result of hepatic IR injury. Whereas the P-gp protein levels in the liver membrane fraction were significantly upregulated after 24 h of IR injury (Fig. 5a), the injury had an opposite effect (a significant reduction) on the liver ATP concentrations (Fig. 4c). Indeed, a reduction in the ATP concentrations during the ischemic period is one of the hallmarks of hepatic IR injury (36). Although the ATP levels recover during the reperfusion period, they may remain below the control levels even 24 h after the reperfusion (37), as observed in our study (Fig. 4c). Because ATP is essential for the function of P-gp, an IR-induced decrease in the ATP concentration (Fig. 4c) could have nullified the observed increase in the protein concentrations of the transporter in the liver (Fig. 5a).

In addition to the decreased ATP concentrations, our studies revealed a significant decrease in the liver: plasma concentration of RH-123 as a result of IR injury (Fig. 4b), suggesting an IR-induced decrease in the hepatic uptake of RH-123. Although it is generally believed that RH-123 enters the cells by passive diffusion, it has been reported that in hepatocytes, Oatp1a4 contributes to the sinusoidal uptake of RH-123 (38). Additionally, a recent study in transfected human embryonic kidney cells showed that RH-123 is subject to facilitated transport via human OATP1A2, which is analogous to rat Oatp1a4 (39). Therefore, we further investigated the effects of hepatic IR on the Oatp1a4 protein content of the liver membrane fraction. The observed decrease in the protein levels of Oatp1a4 in the liver membrane fraction (Fig. 5c) is in agreement with the reduced liver tissue: plasma ratio of the marker (Fig. 4b), confirming an IR-induced reduction in the sinusoidal uptake of RH-123. Collectively, our data suggest that the IR-induced reductions in the biliary recovery (Fig. 2e) and apparent clearance (Fig. 2f) of RH-123, despite an increase in the P-gp protein (Fig. 5a), are most likely due to reductions in both the Oatp1a4 protein levels (Fig. 5c) and the ATP concentrations (Fig. 4c), affecting the hepatic uptake and biliary transport of RH-123, respectively.

Because the glucuronidated metabolite of RH-123 (RH-Glu) is specifically transported into the bile by Mrp2, we also investigated the effect of IR on the biliary transport of RH-Glu. Previous studies have reported that normothermic hepatic IR reduces the mRNA (8,14) and protein (13) levels of

Mrp2 in the liver. Our results, which show decreases in the biliary recovery of RH-Glu (Fig. 2g) and Mrp2 protein content of the liver membrane fraction (Fig. 5b) as a result of 24-h IR, are consistent with these literature data. In addition to the decreased Mrp2 protein, the IR-induced decrease in the hepatic ATP concentrations (Fig. 4c) might have also contributed to the decreased biliary recovery of RH-Glu.

Because we did not administer preformed RH-Glu as such, it may be argued that the observed decrease in the biliary excretion of RH-Glu (Fig. 2g) is due to a possible IR-induced decrease in its formation from RH-123. To address the possible effects of hepatic IR on the glucuronidation pathway, we conducted additional studies using umbelliferone, which is a marker of glucuronidation capacity of the liver. We selected umbelliferone for these *in vitro* studies because we are not aware of any studies reporting formation of RH-Glu *in vitro*. Additionally, our own attempts at formation of RH-Glu *in vitro* using liver microsomes in a previous study (25) and liver homogenates in the current study were not successful. Furthermore, although *in vivo* (29) or *ex vivo* (intact liver) (25,30) formation of RH-Glu has been reported in many studies, based on regeneration of RH-123 after hydrolysis of bile or urine samples with glucuronidase, the exact structure and glucuronyltransferase enzyme(s) responsible for its formation remain unknown at this time. Nevertheless, these studies revealed that IR does not significantly affect the glucuronidation of umbelliferone, suggesting that the IR-induced decrease in the biliary excretion of RH-Glu (Fig. 2g) is most likely not related to a decrease in its formation.

In addition to transporting a number of xenobiotics and their glucuronidated metabolites, Mrp2 also transports glutathione into the bile, which is the main driving force for the bile salt independent bile flow (BIBF) (14). A recent report (40) showed that a short-term (20 min) partial hepatic ischemia followed by 60 min of reperfusion caused internalization of Mrp2 from the bile canalicular membrane, causing a reduction in BIBF. Therefore, the reduction in the Mrp2 protein content in the 24 h IR livers in our study (Fig. 5b) might have been responsible, at least in part, for the reductions in the bile flow rate observed in these animals (Fig. 2h).

The amount of RH-123 recovered in the bile of the 24-h groups during the 40-min sampling period (<4% of dose; Fig. 2e) was low relative to the amount of the marker recovered in the liver tissue at 40 min (23% of dose; Fig. 4a). This is most likely due to the fact that RH-123, a cationic dye, is trapped in the mitochondria in the liver tissue (30). Therefore, only a small fraction of the intracellular RH-123 is freely available for excretion into the bile.

Similar to the upregulation of P-gp protein observed in the liver, the 24-h hepatic IR also caused a significant increase in the P-gp protein content in the brain membrane fraction (Fig. 6a), which is in agreement with a lower K_{in} value for RH-123 in IR animals, compared with the Sham group (Fig. 3f). Upregulation of P-gp in the ischemic and/or remote organs has been reported before in the case of increased hepatic and intestinal P-gp protein after hepatic IR injury (12) or increased intestinal P-gp after intestinal IR (41). However, to the best of our knowledge, our study is the first to report upregulation of P-gp in the brain after IR injury in a peripheral organ. Recent (42–44) *in vitro* works in the area of brain P-gp modulation by proinflammatory mediators have shown that whereas a short-term (<4 h) exposure of the brain capillaries of rats to the inflammatory mediators LPS or TNF-α causes a rapid and reversible decrease in the functional activity of P-gp, a longer-term exposure causes an increased activity and protein expression of the transporter. After hepatic IR, the concentrations of both LPS (4) and TNF-α (45) are elevated in the systemic circulation. Therefore, the higher protein content (Fig. 6a) and activity (decreased K_{in} of RH-123, Fig. 3f) of P-gp at the BBB observed in our IR rats are in agreement with these *in vitro* studies.

Although more polar than RH-123, the metabolite RH-110 showed K_{in} values (~3 μl/min/g) that were comparable to those of the parent drug RH-123 (~3-4 μl/min/g) in the Sham animals (Fig. 3). This is most likely due to the fact that, in contrast to the parent drug, RH-110 is not subject to P-gp efflux. Therefore, an expected reduction in its brain permeability, due to higher polarity, is offset by its lack of efflux, resulting in apparently similar K_{in} values for the drug and metabolite. The lack of effect of IR on the K_{in} value of RH-110 (Fig. 3) suggests that the passive permeability of the BBB to this metabolite is not altered by the injury.

The concept of modulation of P-gp at the BBB by a peripheral disease, although novel, has also been reported recently (46) for another peripheral inflammatory process. Seelbach *et al.* (46) demonstrated that λ-carrageenan-induced inflammatory pain in rats caused overexpression of BBB P-gp and reduction in the brain accumulation of the P-gp substrate morphine. Further studies (47) suggested that the λ-carrageenan-induced changes in the activity of P-gp at the BBB was most likely related to changes in the intracellular trafficking of P-gp within the microvascular endothelial cells. Whether the IR-induced increase in the expression and activity of P-gp observed in our studies is due to induction of synthesis of P-gp or changes in the trafficking of P-gp remains to be determined. Nevertheless, further studies are needed to elucidate the mechanisms of IR-induced increases in P-gp protein and activity in both the liver and brain.

Recent studies suggest an abundant presence of Oatp1a4 at the BBB of mice (48) and rats (49). At the BBB, Oatp1a4 is expressed both at the luminal and abluminal sides of the brain capillary endothelial cells (48), transporting many substrates in both directions. However, the net effect of transport by the BBB Oatp1a4 (blood to brain or brain to blood) depends on the substrate (48). We are not aware of any study demonstrating transport of RH-123 by the brain Oatp1a4.

However, because of transport of RH-123 by Oatp1a4 in other cells, it is likely that RH-123 is transported by Oatp1a4 at the BBB. Therefore, we also determined the effect of hepatic IR on the expression of brain Oatp1a4 in our studies. Although the protein contents of Oatp1a4 in the brains of IR rats were 21% higher than those in the Sham animals, this difference did not reach statistical significance ($p = 0.066$) (Fig. 6b). Nevertheless, because of the bidirectional transport function of Oatp1a4 at the BBB, it is not clear whether an IR-induced overexpression of the transporter, even if it were significant, would be additive or antagonistic to the IR-induced overexpression of P-gp (Fig. 6a) and decreased K_{in} of RH-123 (Fig. 3f).

In addition to its use as a marker of canalicular P-gp (21), the use of RH-123 as an *in vivo* marker of P-gp function at the BBB has been validated in previous studies after both inhibition (22,23) and induction (50) of the transporter. Using microdialysis method, Wang *et al.* (22) reported that co-administration of cyclosporine A, a P-gp substrate and inhibitor, significantly increased the brain distribution of RH-123 in rats by 3.6 fold. Similarly, de Lange *et al.* (23) showed that the brain concentrations of RH-123 in the mdr1a (−/−) mice were 4 fold higher than those in the wild type mice after the intravenous injection of the marker. On the other hand, the overexpression of BBB P-gp resulted in more than 50% reduction in the brain distribution of RH-123 in pentylenetetrazole-kindled rats (50). These data indicate that RH-123 is an appropriate *in vivo* marker for detection of both inhibition and induction of P-gp at the BBB.

Although not a primary objective of this work, it is worthwhile to comment on some apparent differences between the 12- and 24-h Sham values. The RH-110: RH-123 AUC ratios (Table I) and the biliary excretion and bile flow rates (Fig. 2) data suggest a reduction of metabolic and excretory functions in the 12-h group, when compared with the 24-h animals. This may be due to a time-dependent effect of Sham surgery by itself, which has also been reported in other studies (28).

For mechanistic studies, we focused on the 24-h IR injury because of the apparent lack of statistical differences between the Sham and IR groups after 12 h of reperfusion (Table I and Figs. 1, 2 and 3). However, it should be acknowledged that the lack of significance in the 12-h groups, at least for some parameters, might be due to a low sample size ($n = 5$), and hence a low statistical power. Nevertheless, as opposed to the 24-h groups, the absolute magnitude of differences between the Sham and IR groups for the 12-h injury were very low for most of the parameters. Indeed, the maximum difference between the Sham and IR groups (~20%) was observed for the apparent biliary clearance of RH-123 (Fig. 2b). Given the extent of variability of the parameter (CV of 26%), a sample size calculation indicated an n of 27 to detect such a difference statistically with a power of 80%, which was not deemed justified. Therefore, additional animals were not added to this group.

CONCLUSIONS

In conclusion, the data presented in this manuscript indicate that the hepatic IR injury alters the expression and function of P-gp in the liver and at the BBB. Whereas P-gp protein and function are increased in the remote organ (brain), the increase in the transporter's protein in the ischemic organ (liver) is accompanied by a decrease in the hepatic concentrations of ATP, thus diminishing the impact of the increased P-gp protein in the liver. In contrast to P-gp overexpression, hepatic IR decreased the protein contents of hepatic sinusoidal Oatp1a4 and canalicular Mrp2. The IR-induced changes in the studied transporters resulted in significant changes in the *in vivo* pharmacokinetics of RH-123 (P-gp and Oatp1a4 substrate) and its metabolite RH-Glu (Mrp2 substrate), including reduction of their biliary recovery and a decrease in the brain uptake clearance of RH-123. These studies suggest that the peripheral pharmacokinetics and brain distribution of drugs that are transported by P-gp, and possibly other transporters, may be altered as a result of hepatic IR injury.

ACKNOWLEDGMENTS AND DISCLOSURES

Mohammad K. Miah and Imam H. Shaik contributed equally to this work. The authors would like to acknowledge financial support from the Blood–brain Barrier Research Center at Texas Tech School of Pharmacy. Additionally, we would like to thank Dr. Thomas J. Thekkumkara for the use of VersaDoc Image System in his laboratory.

REFERENCES

1. Lemasters JJ, Thurman RG. Reperfusion injury after liver preservation for transplantation. Annu Rev Pharmacol Toxicol. 1997;37:327–38.
2. Jaeschke H. Molecular mechanisms of hepatic ischemia-reperfusion injury and preconditioning. Am J Physiol Gastrointest Liver Physiol. 2003;284:G15–26.
3. Zhai Y, Busuttil RW, Kupiec-Weglinski JW. Liver ischemia and reperfusion injury: new insights into mechanisms of innate-adaptive immune-mediated tissue inflammation. Am J Transplant. 2011;11:1563–9.
4. Fiorini RN, Shafizadeh SF, Polito C, Rodwell DW, Cheng G, Evans Z, *et al*. Anti-endotoxin monoclonal antibodies are protective against hepatic ischemia/reperfusion injury in steatotic mice. Am J Transplant. 2004;4:1567–73.
5. Wanner GA, Ertel W, Muller P, Hofer Y, Leiderer R, Menger MD, *et al*. Liver ischemia and reperfusion induces a systemic inflammatory response through Kupffer cell activation. Shock. 1996;5:34–40.
6. Rymsa B, Wang JF, de Groot H. O2-. release by activated Kupffer cells upon hypoxia-reoxygenation. Am J Physiol. 1991;261:G602–7.
7. Liu P, McGuire GM, Fisher MA, Farhood A, Smith CW, Jaeschke H. Activation of Kupffer cells and neutrophils for reactive oxygen

formation is responsible for endotoxin-enhanced liver injury after hepatic ischemia. Shock. 1995;3:56–62.
8. Tanaka Y, Chen C, Maher JM, Klaassen CD. Kupffer cell-mediated downregulation of hepatic transporter expression in rat hepatic ischemia-reperfusion. Transplantation. 2006;82:258–66.
9. Fardel O, Le Vee M. Regulation of human hepatic drug transporter expression by pro-inflammatory cytokines. Expert Opin Drug Metab Toxicol. 2009;5:1469–81.
10. Geier A, Dietrich CG, Voigt S, Kim SK, Gerloff T, Kullak-Ublick GA, *et al*. Effects of proinflammatory cytokines on rat organic anion transporters during toxic liver injury and cholestasis. Hepatology. 2003;38:345–54.
11. Hartmann G, Cheung AK, Piquette-Miller M. Inflammatory cytokines, but not bile acids, regulate expression of murine hepatic anion transporters in endotoxemia. J Pharmacol Exp Ther. 2002;303:273–81.
12. Ikemura K, Urano K, Matsuda H, Mizutani H, Iwamoto T, Okuda M. Decreased oral absorption of cyclosporine A after liver ischemia-reperfusion injury in rats: the contribution of CYP3A and P-glycoprotein to the first-pass metabolism in intestinal epithelial cells. J Pharmacol Exp Ther. 2009;328:249–55.
13. Tanaka Y, Chen C, Maher JM, Klaassen CD. Ischemia-reperfusion of rat livers decreases liver and increases kidney multidrug resistance associated protein 2 (Mrp2). Toxicol Sci. 2008;101:171–8.
14. Fouassier L, Beaussier M, Schiffer E, Rey C, Barbu V, Mergey M, *et al*. Hypoxia-induced changes in the expression of rat hepatobiliary transporter genes. Am J Physiol Gastrointest Liver Physiol. 2007;293: G25–35.
15. Parasrampuria R, Shaik IH, Mehvar R. Effects of in vivo hepatic ischemia-reperfusion injury on the hepatobiliary disposition of rhodamine 123 and its metabolites in isolated perfused rat livers. J Pharm Pharm Sci. 2012;15:318–28.
16. Syvanen S, Lindhe O, Palner M, Kornum BR, Rahman O, Langstrom B, *et al*. Species differences in blood-brain barrier transport of three positron emission tomography radioligands with emphasis on P-glycoprotein transport. Drug Metab Dispos. 2009;37: 635–43.
17. Agarwal S, Elmquist WF. Insight into the cooperation of P-glycoprotein (ABCB1) and breast cancer resistance protein (ABCG2) at the blood-brain barrier: a case study examining sorafenib efflux clearance. Mol Pharm. 2012;9:678–84.
18. Miller DS. Regulation of P-glycoprotein and other ABC drug transporters at the blood-brain barrier. Trends Pharmacol Sci. 2010;31: 246–54.
19. Kusuhara H, Sugiyama Y. Efflux transport systems for drugs at the blood-brain barrier and blood-cerebrospinal fluid barrier (Part 2). Drug Discov Today. 2001;6:206–12.
20. Syvanen S, Xie R, Sahin S, Hammarlund-Udenaes M. Pharmacokinetic consequences of active drug efflux at the blood-brain barrier. Pharm Res. 2006;23:705–17.
21. Ando H, Nishio Y, Ito K, Nakao A, Wang L, Zhao YL, *et al*. Effect of endotoxin on P-glycoprotein-mediated biliary and renal excretion of rhodamine-123 in rats. Antimicrob Agents Chemother. 2001;45: 3462–7.
22. Wang Q, Yang H, Miller DW, Elmquist WF. Effect of the p-glycoprotein inhibitor, cyclosporin A, on the distribution of rhodamine-123 to the brain: an in vivo microdialysis study in freely moving rats. Biochem Biophys Res Commun. 1995;211:719–26.
23. de Lange EC, de Bock G, Schinkel AH, de Boer AG, Breimer DD. BBB transport and P-glycoprotein functionality using MDR1A (-/-) and wild-type mice. Total brain versus microdialysis concentration profiles of rhodamine-123. Pharm Res. 1998;15:1657–65.
24. Stapf V, Thalhammer T, Huber-Huber R, Felberbauer F, Gajdzik L, Graf J. Inhibition of rhodamine 123 secretion by cyclosporin A as a model of P-glycoprotein mediated transport in liver. Anticancer Res. 1994;14:581–5.
25. Parasrampuria R, Mehvar R. Effects of P-glycoprotein and Mrp2 inhibitors on the hepatobiliary disposition of Rhodamine 123 and its glucuronidated metabolite in isolated perfused rat livers. J Pharm Sci. 2010;99:455–66.
26. Shaik IH, Mehvar R. Cytochrome P450 induction by phenobarbital exacerbates warm hepatic ischemia-reperfusion injury in rat livers. Free Radic Res. 2010;44:441–53.
27. Spiegel HU, Bahde R. Experimental models of temporary normothermic liver ischemia. J Investig Surg. 2006;19:113–23.
28. Shaik IH, Mehvar R. Effects of normothermic hepatic ischemia-reperfusion injury on the in vivo, isolated perfused liver, and microsomal disposition of chlorzoxazone, a cytochrome P450 2E1 probe, in rats. J Pharm Sci. 2011;100:5281–92.
29. Sweatman TW, Seshadri R, Israel M. Metabolism and elimination of rhodamine 123 in the rat. Cancer Chemother Pharmacol. 1990;27: 205–10.
30. Parasrampuria R, Mehvar R. Hepatobiliary disposition of rhodamine 123 in isolated perfused rat livers. Xenobiotica. 2008;38:1263–73.
31. Lee KJ, Mower R, Hollenbeck T, Castelo J, Johnson N, Gordon P, *et al*. Modulation of nonspecific binding in ultrafiltration protein binding studies. Pharm Res. 2003;20:1015–21.
32. Manfredi G, Yang L, Gajewski CD, Mattiazzi M. Measurements of ATP in mammalian cells. Methods. 2002;26:317–26.
33. Vuppugalla R, Mehvar R. Selective effects of nitric oxide on the disposition of chlorzoxazone and dextromethorphan in isolated perfused rat livers. Drug Metab Dispos. 2006;34:1160–6.
34. Killard AJ, O'Kennedy R, Bogan DP. Analysis of the glucuronidation of 7-hydroxycoumarin by HPLC. J Pharm Biomed Anal. 1996;14:1585–90.
35. Bickel U. How to measure drug transport across the blood-brain barrier. NeuroRx. 2005;2:15–26.
36. Bedirli N, Ofluoglu E, Kerem M, Utebey G, Alper M, Yilmazer D, *et al*. Hepatic energy metabolism and the differential protective effects of sevoflurane and isoflurane anesthesia in a rat hepatic ischemia-reperfusion injury model. Anesth Analg. 2008;106:830–7.
37. Ofluoglu E, Kerem M, Pasaoglu H, Turkozkan N, Seven I, Bedirli A, *et al*. Delayed energy protection of ischemic preconditioning on hepatic ischemia/reperfusion injury in rats. Eur Surg Res. 2006;38: 114–21.
38. Annaert PP, Brouwer KL. Assessment of drug interactions in hepatobiliary transport using rhodamine 123 in sandwich-cultured rat hepatocytes. Drug Metab Dispos. 2005;33:388–94.
39. Forster S, Thumser AE, Hood SR, Plant N. Characterization of rhodamine-123 as a tracer dye for use in in vitro drug transport assays. PLoS ONE. 2012;7:e33253.
40. Ban D, Kudo A, Sui S, Tanaka S, Nakamura N, Ito K, *et al*. Decreased Mrp2-dependent bile flow in the post-warm ischemic rat liver. J Surg Res. 2009;153:310–6.
41. Omae T, Goto M, Shimomura M, Masuda S, Ito K, Okuda M, *et al*. Transient up-regulation of P-glycoprotein reduces tacrolimus absorption after ischemia-reperfusion injury in rat ileum. Biochem Pharmacol. 2005;69:561–8.
42. Hartz AM, Bauer B, Fricker G, Miller DS. Rapid modulation of P-glycoprotein-mediated transport at the blood-brain barrier by tumor necrosis factor-alpha and lipopolysaccharide. Mol Pharmacol. 2006;69:462–70.
43. Bauer B, Hartz AM, Miller DS. Tumor necrosis factor alpha and endothelin-1 increase P-glycoprotein expression and transport activity at the blood-brain barrier. Mol Pharmacol. 2007;71: 667–75.
44. Rigor RR, Hawkins BT, Miller DS. Activation of PKC isoform beta(I) at the blood-brain barrier rapidly decreases P-glycoprotein activity and enhances drug delivery to the brain. J Cereb Blood Flow Metab. 2010;30:1373–83.

45. Peralta C, Fernandez L, Panes J, Prats N, Sans M, Pique JM, *et al*. Preconditioning protects against systemic disorders associated with hepatic ischemia-reperfusion through blockade of tumor necrosis factor-induced P-selectin up-regulation in the rat. Hepatology. 2001;33:100–13.
46. Seelbach MJ, Brooks TA, Egleton RD, Davis TP. Peripheral inflammatory hyperalgesia modulates morphine delivery to the brain: a role for P-glycoprotein. J Neurochem. 2007;102:1677–90.
47. McCaffrey G, Staatz WD, Sanchez-Covarrubias L, Finch JD, Demarco K, Laracuente ML, *et al.* P-glycoprotein trafficking at the blood-brain barrier altered by peripheral inflammatory hyperalgesia. J Neurochem. 2012; 122:962–75.
48. Ose A, Kusuhara H, Endo C, Tohyama K, Miyajima M, Kitamura S, *et al*. Functional characterization of mouse organic anion transporting peptide 1a4 in the uptake and efflux of drugs across the blood-brain barrier. Drug Metab Dispos. 2010;38: 168–76.
49. Ronaldson PT, Finch JD, Demarco KM, Quigley CE, Davis TP. Inflammatory pain signals an increase in functional expression of organic anion transporting polypeptide 1a4 at the blood-brain barrier. J Pharmacol Exp Ther. 2011;336:827–39.
50. Liu X, Yang Z, Yang J, Yang H. Increased P-glycoprotein expression and decreased phenobarbital distribution in the brain of pentylenetetrazole-kindled rats. Neuropharmacology. 2007;53:657–63.